Journal of Neuroscience Research 62:530–538 (2000)

Extracellular Diffusion Parameters in Spinal Cord and Filum Terminale of the Frog

Šárka Prokopová-Kubinová[1,2] **and Eva Syková**[1,2]*
[1]Department of Neuroscience, Second Medical Faculty, Charles University, Prague, Czech Republic
[2]Institute of Experimental Medicine, Academy of Sciences of the Czech Republic, Prague, Czech Republic

Extracellular space (ECS) diffusion parameters were studied in isolated frog spinal cord grey matter and filum terminale (FT), that is predominantly composed of glial cells and axons. We compared the cell swelling induced by K^+ application, hypotonic stress and tetanic stimulation of afferent input. The ECS diffusion parameters, volume fraction α (α = ECS volume/total tissue volume), tortuosity λ (λ^2 = free/apparent diffusion coefficient in the tissue) and non-specific cellular uptake k', were determined by the real-time iontophoretic method using TMA^+-selective microelectrodes. Stimulation-evoked changes in extracellular K^+ concentration ($[K^+]_e$) were measured by K^+-selective microelectrodes. Histological analysis revealed that in the central region of the FT, the cell density was lower than in SC, neurons and oligodendrocytes were scarce, GFAP-positive astrocytes were abundant, and they showed thicker and more densely stained processes than in spinal cord. In the FT, α was 58% higher and λ significantly lower than in the spinal cord. In 50 mM K^+, α in spinal cord decreased from about 0.19 to 0.09, i.e., by 53%, whereas in FT from about 0.32 to 0.20, i.e., by only 38%; λ increased significantly more in FT than in spinal cord. Hypotonic solution (175 mmol/kg^{-1}) resulted in similar decreases in α, and there were no changes in λ in either spinal cord or FT. Stimulation of VIII or IX dorsal root (DR) by 30 Hz evoked an increase in $[K^+]_e$ from 3 to 11–12 mM in spinal cord, but to only 4–5 mM in FT. In the spinal cord this stimulation led to a 30% decrease in α and a small increase in λ whereas in the FT the decrease in α was only about 10% and no increase in λ was found. We conclude that in spinal cord, a complex tissue with a higher density of cellular elements than the FT, 50 mM K^+, hypotonic stress as well as DR stimulation evoked a greater decrease in ECS volume than in FT. Nevertheless, the K^+-induced increase in tortuosity was higher in FT, suggesting that a substantial part of the K^+-evoked increase in λ was due to astrocytic swelling. J. Neurosci. Res. 62: 530–538, 2000. © 2000 Wiley-Liss, Inc.

Key words: amphibian; stimulation; cell swelling; astrocytes; oligodendrocytes; neurons

The size, composition and geometry of the extracellular space (ECS) determine the diffusion of substances in the brain and play an important role in extrasynaptic or volume transmission (Fuxe and Agnati, 1991; Syková, 1997; Nicholson and Syková, 1998, Zoli et al., 1999). This type of signal transmission takes place in short- and long-distance communication between neurons and neurons and glia. It is significantly affected during pathological states, when cellular swelling occurs due to transmembrane ionic shifts and water movement from the extra- to the intracellular compartment (Syková, 1997). This cellular swelling not only causes a decrease in ECS volume but also induces changes in ECS geometry and therefore hinders the movement of substances through the ECS. There is some evidence that astrogliosis may play an important role in volume transmission by the formation of ECS diffusion barriers (Roitbak and Syková, 1999; Syková et al., 1999), but it is not clear what is the mechanism underlying the increase in tortuosity observed during cell swelling.

Diffusion in the ECS of the neural tissue obeys Ficks' law, but it is constrained by three factors (Nicholson and Phillips, 1981): the extracellular space volume fraction α (α = ECS volume/total tissue volume); the tortuosity λ (λ^2 = free/apparent diffusion coefficient in the tissue), a factor that describes how the migration of molecules is slowed down by various obstructions including neuronal and glial processes, electrical charges and macromolecules of the extracellular matrix; and non-specific uptake k', a factor describing the loss of material across cell membranes. Using the real-time iontophoretic method, that employs ion-selective microelectrodes to follow the diffusion of extracellular markers applied by iontophoresis, the absolute values of the three ECS diffusion parameters can be determined (Nicholson and Phillips, 1981; Nicholson and Syková, 1998). The isolated spinal cord has been shown to maintain the same diffusion parameter values as the spinal cord in vivo (Prokopová et al., 1997; Syková et al., 1999).

It has been shown that during repetitive neuronal activity in the frog as well as the rat spinal cord, the ECS diffusion parameters change, presumably due to activity-

Contract grant sponsor: GAČR; Contract grant numbers: 309/99/0657, 309/97/K048, 307/96/K226; Contract grant sponsor: VS; Contract grant number: 96-130.

*Correspondence to: Eva Syková, MD, PhD, DSc, Department of Neuroscience, Institute of Experimental Medicine ASCR, Vídeňská 1083, 142 20 Prague 4, Czech Republic. E-mail: sykova@biomed.cas.cz

Received 25 April 2000; Revised 13 July 2000; Accepted 21 July 2000

related cell swelling (Svoboda and Syková, 1991). A transient increase in extracellular K^+ concentration in the range of 6–50 mM accompanies nociceptive stimulation, repetitive electrical stimulation and many pathological states (Syková, 1987; Chvátal et al., 1988; Svoboda et al., 1988). The bath elevation of extracellular K^+ concentration also leads to an ECS volume decrease due to the cellular accumulation of ions and water (Ritchie et al., 1981; Kimelberg and Frangakis, 1985; Walz and Hinks, 1985; Syková et al., 1999) and to a tortuosity increase, presumably due to the swelling of glial processes (Roitbak and Syková, 1999). Our previous studies in rat revealed that the cellular swelling evoked by hypotonic solution or high K^+ results in different changes in the ECS diffusion parameters (Syková et al., 1999). K^+-induced swelling is mostly attributed to glia (Kimelberg and Ransom, 1986), but swelling of neuronal elements has also been suggested (Van Harreveld and Khattab, 1967). It is therefore not clear to what extent glial and neuronal swelling affect diffusion properties of the ECS under such different conditions as neuronal activity, K^+ accumulation and hypotonic stress. Moreover, the tortuosity is influenced by many factors that we cannot easily separate. To elucidate these questions we used the filum terminale of the frog spinal cord that is a persistent remnant after larval tail absorption and is mainly composed of astroglia. The presumed predominance of the glial elements and the loss of their functional relationship with neurons (Glusman et al., 1979; Ritchie et al., 1981) make this tissue a useful preparation for our study. In this study all three ECS diffusion parameters and the changes evoked by elevated K^+, hypotonic stress or repetitive electrical stimulation were examined, in both the spinal dorsal horn and in the filum terminale.

MATERIAL AND METHODS

Animal Preparation and Stimulation

The frogs (*Rana pipiens*, WA Lamberger Inc., Oshkosh, WI) were decapitated under ether anesthesia, and the spinal cord was dissected in a chamber with cold (9–11°C) Ringer solution of the following composition (in mM): NaCl 114.0, KCl 3.0, $NaHCO_3$ 20.0, $CaCl_2$ 1.8, D-glucose 10.0 (Syková et al., 1976). In experiments using TMA^+-selective microelectrodes, the Ringer solution contained 0.1 mM TMA^+. The isolated cord was mounted in a chamber, and the preparation was continuously superfused with Ringer solution, saturated with 95% O_2 and 5% CO_2 (pH 7.3) at a flow rate of 10 ml/min. During 30–60 min the temperature was increased to 17–19°C and maintained there throughout the experiment. The VIII or IX dorsal roots (DR) were stimulated supramaximally (rectangular pulses of 10 V; duration 0.1 msec) with a fine bipolar silver electrode (Syková et al., 1976). Changes in $[K^+]_e$ activity were measured by means of double-barreled ion-sensitive microelectrodes filled with a K^+ liquid ion-exchanger (Corning 477317). Hypoosmotic solutions were prepared by reducing the NaCl content. The osmotic strength of the solutions was measured with a vapor pressure osmometer. The Ringer solution had an osmolality of 270 mmol/kg, hypotonic solution 175 mmol/kg. Solutions with an increased K^+ or Mg^{2+} concentration had a reciprocally reduced Na^+ concentration. In the spinal cord, the measurements were performed in the dorsal horn grey matter of the lumbar enlargement. The array of electrodes was lowered into the spinal cord from the dorsal spinal surface, about 250 μm laterally from the midline, to a depth of 300–350 μm. In the filum terminale, that is the terminal portion of the spinal cord extending caudally beyond the level of the last spinal root, the measurements of ECS diffusion parameters were performed in the intermediate zone, about 100 μm laterally from the midline at a depth of 200–250 μm from the dorsal surface. The measurements were performed in two areas: FT I, located 1–2 mm and FT II, located 2–3 mm below the entry zone of the last dorsal root.

Measurement of ECS Diffusion Parameters

The ECS diffusion parameters were studied by means of the iontophoretic application of an extracellular marker, TMA^+ (MW 74.1), to which cellular membranes are relatively impermeable. The concentration of TMA^+ in the ECS, measured by TMA^+-selective microelectrodes (TMA^+-ISM), is inversely proportional to the ECS volume. The TMA^+-selective microelectrodes were made from double-barreled glass tubing as described in detail elsewhere (Kříž et al., 1975). The ion-sensing barrel containing Corning 477317 ion-exchanger was backfilled with 100 mM TMA-chloride. Electrodes were calibrated before and after each experiment in solutions of 150 mM NaCl + 3 mM KCl with the addition of the following amounts of TMA-chloride (in mM): 0.03, 0.1, 0.3, 1.0, 3.0, 10.0.

Iontophoresis pipettes were prepared from theta glass. The shank was bent before back-filling with 100 mM TMA-chloride, so that it could be aligned parallel to that of the TMA^+-ISM. Electrode arrays were made by gluing together an iontophoresis pipette and a TMA^+-ISM with a tip separation of 100–200 μm (Fig. 1A). The iontophoresis parameters were +20 nA bias current (continuously applied to maintain a constant transport number), with an +80 nA current step of 60 sec duration to generate the diffusion curve. TMA^+ diffusion curves were analyzed by fitting the data to a solution of the diffusion equation (Nicholson and Phillips, 1981). Before the measurements were performed in the tissue, concentration-versus-time curves for TMA^+ diffusion were recorded in 0.3% agar gel (Difco, USA) dissolved in a solution of 150 mM NaCl, 3 mM KCl and 1 mM TMA-chloride to determine the transport number (n) and the free TMA^+ diffusion coefficient (D).

Immunohistochemistry

Isolated spinal cords were fixed with 4% paraformaldehyde in 0.1 M phosphate-buffered saline (PBS; pH 7.5) for 4 hr, trimmed, then immersed in PBS containing 30% sucrose. Frozen transverse section (40 μm) were cut through the lumbar part of the spinal cord and through the filum terminale. Selected sections were stained by Nissl staining using cresyl violet whereas others were immunostained for neurofilaments, astrocytes, oligodendrocytes and myelin.

Nissl staining using cresyl violet was used to measure the numeric density of cellular bodies in spinal cord and filum terminale. Nine slices of each tissue were examined by a Leica

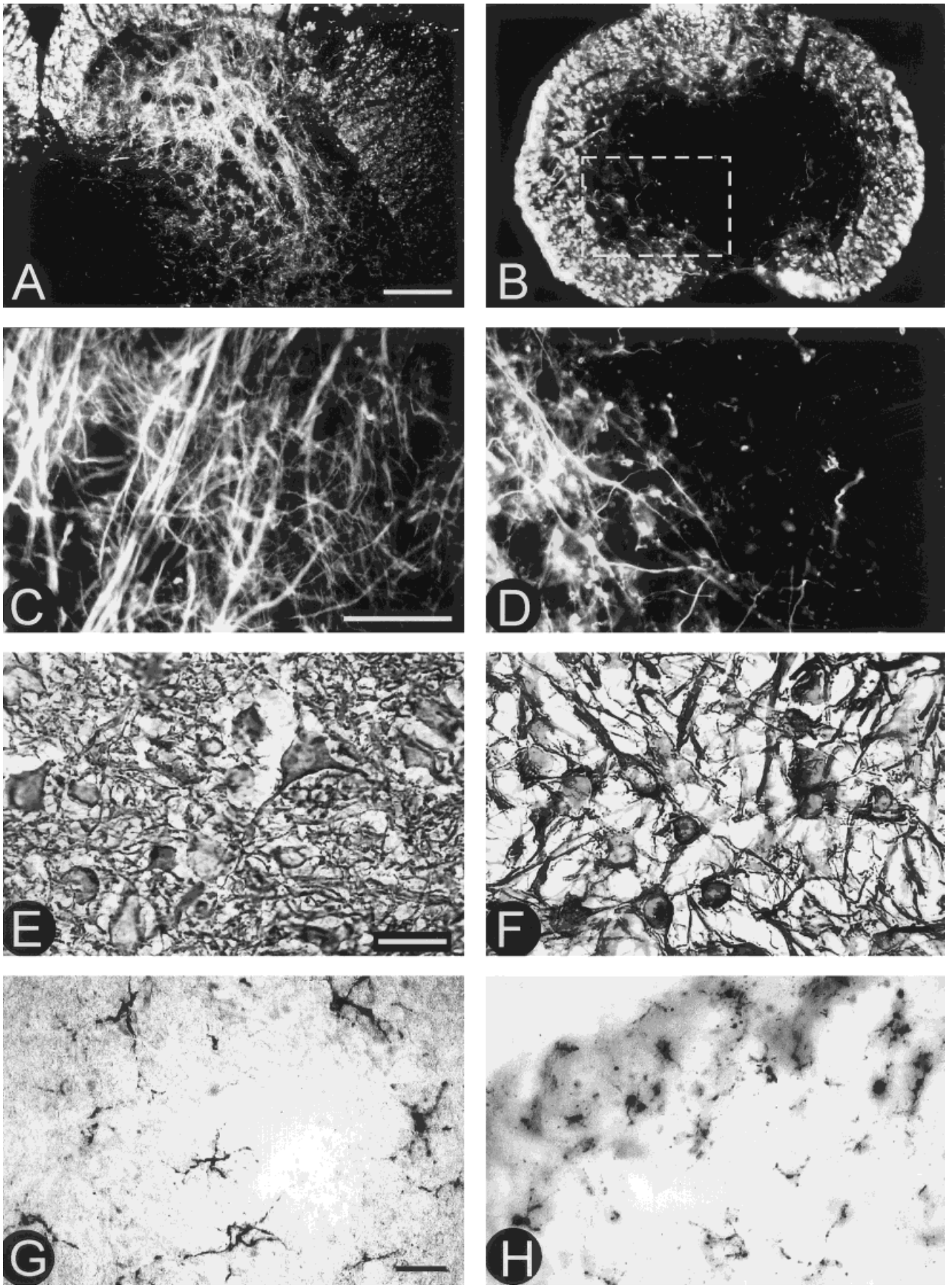

Figure 1.

Image Analysis System to determine the number of cells in the selected fields (450 × 350 μm), that were located in the dorsal horn of the spinal cord or in the intermediate zone of the filum terminale II. The density was then recalculated to an area of 0.1 mm^2.

Neurofilaments were identified using antibodies against 200 kD neurofilaments (Boehringer-Mannheim). Primary antibodies were diluted to 0.4–0.8 μg/ml in PBS containing 1% bovine serum albumin (BSA, Sigma) and 0.2% Triton X-100. After overnight incubation in the primary antibodies at 4°C, the floating sections were washed and processed by using anti-mouse secondary antibodies and Texas Red Avidin (Vector Laboratories). Astrocytes were identified using polyclonal rabbit antibodies to GFAP (Boehringer-Mannheim). GFAP antibodies were diluted to 0.4 μg/ml in PBS containing 1% BSA (Sigma) and 0.2% Triton X-100. Oligodendrocytes and myelin were immunostained with Rip a monoclonal antibody specific for oligodendroglia and central myelin (courtesy of Friedman University of Iowa; see Friedman et al., 1989). The partially purified Rip supernatant was diluted 1:50 in PBS with 1% BSA and 0.2% Triton X-100 added. After overnight incubation in the primary antibodies at 4°C, the floating sections were washed and processed by using secondary antibodies and the peroxidase-labeled avidin-biotin complex method (Vectastain Elite, Vector Laboratories). Immune complexes were visualized using 0.05% 3.3′-diaminobenzidine tetrachloride (Sigma) in PBS and 0.02% H_2O_2.

Statistical Analysis

All data are expressed as mean ± SEM. The statistical significance of data was evaluated by two-tailed one-way ANOVA (SigmaStat 2.0, Jandel Scientific). Significance was accepted at $P < 0.05$.

RESULTS

Immunohistochemistry

The filum terminale is considered to be that portion of the spinal cord extending caudally beyond the entry zone of the last spinal dorsal root. It is composed of glia, myelinated and unmyelinated fibers and degenerated neurons (Gonzáles-Robles and Glusman, 1979). The rostral portion of the filum terminale (FT I) resembles the upper regions of the frog spinal cord with myelinated fibers in the peripheral region. The number of myelinated fibers as well as the density of cellular elements diminish in the most caudal regions (FT II) compared with the rostral portion.

Using Nissl staining, the numeric density of cell bodies in the dorsal horn grey matter of the lumbar enlargement was 180 ± 6/0.1 mm^2, that was significantly higher than the density in the FT II, 126 ± 13/0.1 mm^2 (n = 9, $P < 0.001$). Compared to spinal cord there was clearly a lower density of the cellular network, that could result in a larger extracellular space.

Immunostaining for neurofilaments revealed their presence in the spinal cord grey as well as white matter (Fig. 1A). In the grey matter the neurofilaments created a dense network between the cell bodies. In white matter the neurofilaments were usually cut transversally, as the staining revealed cross-sections of axons. The neurofilaments in both FT I and FT II were present in the peripheral part only (Fig. 1B), also seen as axonal cross-sections as in spinal cord white matter, and were absent in the more central part. Higher magnification (Fig. 1C,D) showed that the neurofilaments in spinal cord grey matter were thicker than those in filum terminale. The neurofilaments in filum terminale were thin and sparse.

GFAP staining for astrocytes in the spinal cord grey matter showed fine astrocytic processes forming a dense network (Fig. 1E). In the filum terminale, particularly in its intermediate zone, the astrocyte bodies were larger and their processes were densely stained and thick (Fig. 1F). Rip staining revealed in the spinal cord oligodendrocytes with several fine and long processes, mostly present in the grey matter of the ventral horns. In the filum terminale the oligodendrocytes were stained in the peripheral as well as the intermediate parts. The processes were stained less intensely and were shorter than those in the spinal cord (Fig.1G,H).

ECS Diffusion Parameters

ECS diffusion parameters in the spinal cord dorsal horn differed from those in the FT. Figure 2B shows typical diffusion curves recorded in the spinal cord dorsal horn and in the FT. α in the FT was about 66% higher and λ about 12% lower than in the spinal cord. In the spinal cord, the mean value of the ECS volume fraction α = 0.19 and tortuosity λ = 1.59, whereas in the FT I and FT II α = 0.31 and 0.32 and λ = 1.40 and 1.43, respectively (Table I). We found no significant differences in ECS diffusion parameters between FT I and FT II with the exception that non-specific uptake in the FT II was significantly higher than in the spinal cord.

Fig. 1. Distribution of neurofilaments as revealed by anti-200 kDa neurofilament antibody; the neurofilaments can be seen in the white and grey matter of the spinal cord (**A**) but only in the peripheral regions of the filum terminale (**B**). Higher magnification shows a dense network of neurofilaments in the grey matter of the spinal dorsal horn (**C**) and sparse neurofilaments in the central region and thinner neurofilaments in the peripheral region (the rectangle in B) of the filum terminale (**D**). Astrocytes stained for GFAP in dorsal spinal horn (**E**) and the intermediate part of the filum terminale (**F**). Note the thicker and more densely stained processes in the filum terminale, but forming a less dense network than in the spinal dorsal horn. **G,H:** oligodendrocytes stained with Rip antibody. The oligodendrocytes are densely stained in the grey matter of the ventral horns and reveal several fine processes. The oligodendrocytes in the filum terminale have shorter processes and are present mostly in the peripheral region, not defined as white matter. Scale bars = 100 μm in A (also applies to B); 50 μm in C (also applies to D); 20 μm in E (also applies to F); 20 μm in G (also applies to H).

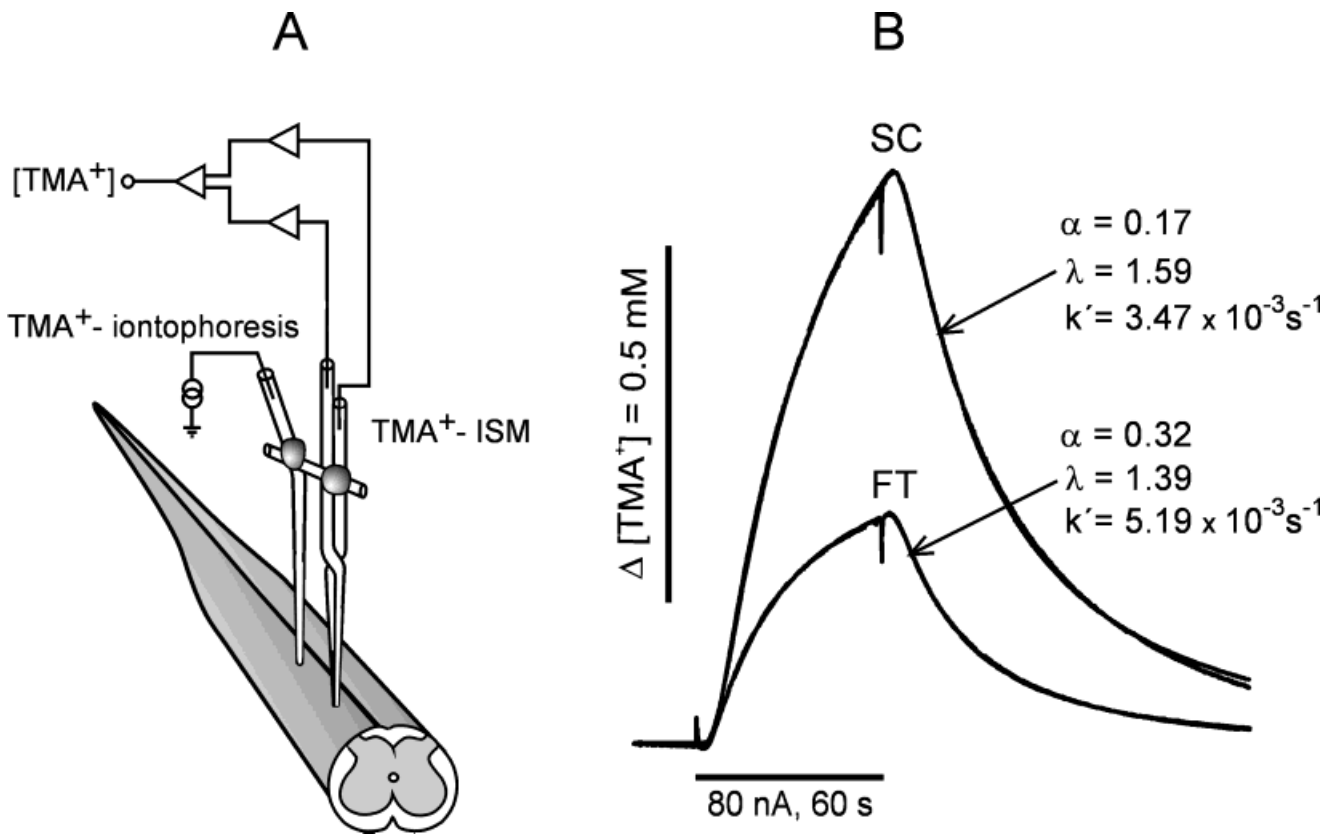

Fig. 2. Experimental set-up and representative diffusion curves obtained in the spinal cord and filum terminale. **A:** The experimental arrangement. A TMA^+-selective double-barreled ion-selective microelectrode (ISM) was glued to an iontophoresis microelectrode. The separation between electrode tips was 100–200 μm. When the electrode array was inserted into the spinal cord and the iontophoretic current applied, the diffusion curve resulting from the increase in TMA^+ concentration was measured in the spinal dorsal horn (SC) and in the filum terminale I. **B:** Recordings obtained in SC and FT. The values for volume fraction (α), tortuosity (λ) and non-specific uptake (k') are shown with each curve. The microelectrode array spacing was 170 μm and n = 0.25. Both diffusion curves were recorded in the same animal.

TABLE I. ECS Diffusion Parameters in the Frog Spinal Cord and Filum Terminale†

Structure	n	α	λ	k′ (10^{-3} s^{-1})
Spinal cord	35	0.19 ± 0.01	1.59 ± 0.01	3.95 ± 0.32
Filum terminale I	13	0.31 ± 0.01⋆	1.40 ± 0.02⋆	4.24 ± 0.46
Filum terminale II	13	0.32 ± 0.01⋆	1.43 ± 0.01⋆	5.57 ± 0.58⋆

†Data are expressed as mean ± SEM; n is the number of animals. Statistical analysis of the differences between spinal cord and filum terminale I or II was performed by ANOVA test.
⋆$P < 0.05$.

Effect of Elevated K^+ and Hypotonic Stress on Diffusion Parameters in Spinal Cord and Filum Terminale

The effect of 50 mM K^+ and hypotonic stress was studied in dorsal horn grey matter and FT I. The application of 50 mM K^+ (Fig. 3A) for 40 min led, in both spinal cord and FT, to changes in α and λ. α decreased in spinal cord to 0.09 ± 0.01 (n = 6), i.e., by 53%, in FT to 0.20 ± 0.02 (n = 6), i.e., by 35%. λ in spinal cord increased from 1.60 ± 0.02 to 1.70 ± 0.04, i.e., by 6%, whereas in FT the increase was greater, from 1.39 ± 0.03 to 1.68 ± 0.02, i.e., by 21% ($P < 0.005$). The application of hypotonic solution (175 mmol/kg) (Fig. 3B) for 40 min resulted in a decrease in α to 0.11 ± 0.02 (n = 4) in the spinal cord, i.e., by 42%. In the FT α decreased to 0.22 ± 0.01 (n = 4), i.e., by only 29%. In both structures, the small changes in λ were not significant.

It is therefore evident that in elevated K^+ as well as in hypotonic solution, the relative decrease in α was greater in spinal cord than in FT. The increase in λ evoked by 50 mM K^+, however, was higher in the FT than in spinal cord, suggesting that astrocytes play an important role in the increase of diffusion barriers during pathological states.

Stimulation-Evoked Changes in Extracellular K^+ Activity and Diffusion Parameters

ECS volume changes and tortuosity were studied during and after electrical stimulation of the VIII or IX

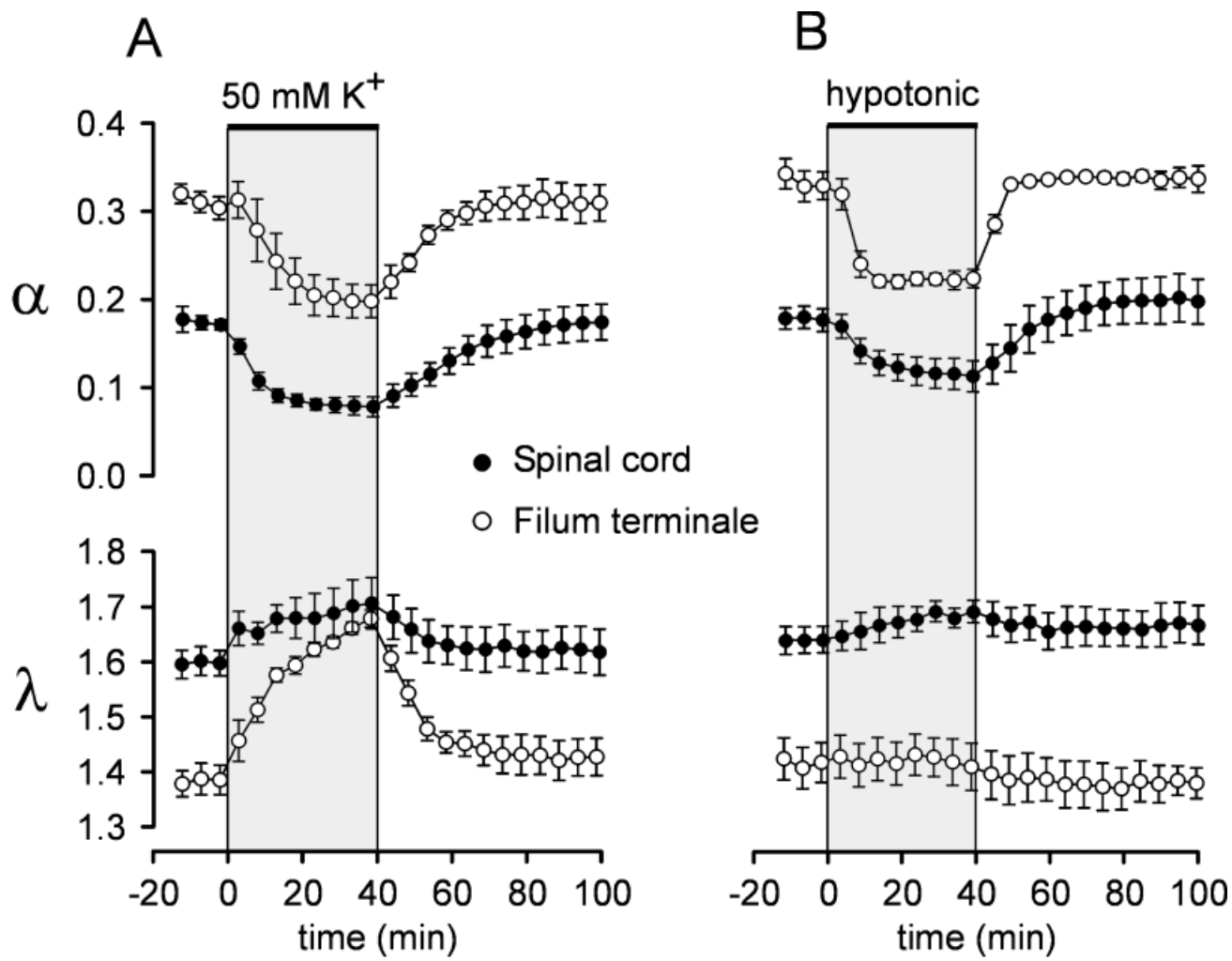

Fig. 3. The effect of 50 mM K^+ and hypotonic solution in spinal cord and filum terminale I. Each data point (mean ± SEM) was calculated from α and λ values recorded at 5 min intervals from six (**A**) and four (**B**) experiments. The application of 50 mM K^+ (A) resulted in a greater decrease in α in FT than in spinal cord. The increase in λ was significantly higher in FT than in spinal cord. Hypotonic solution (175 mmol/kg) (B) also resulted in a greater decrease in α in FT than in spinal cord, with no significant increase in λ in either spinal cord or FT.

dorsal root. Tetanic stimulation at 30 Hz lasting for 5 or 30 min produced an increase in $[K^+]_e$ of 8–9 mM in spinal dorsal horn (Fig. 4A,B). This increase was accompanied by a concomitant reduction in the size of the ECS (Fig. 4E,F). There was a close relationship between the time course of the evoked $[K^+]_e$ increase and the ECS shrinkage. During the first 30 sec of electrical stimulation, $[K^+]_e$ rose by 8–9 mM and α decreased from about 0.18 to 0.13, i.e., by about 27%. Further stimulation did not lead to a further increase in $[K^+]_e$, i.e., the so-called "ceiling level" was reached, apparently because a balance is established between the release and redistribution of accumulated K^+ (Syková et al., 1988). Similarly, the ECS volume did not decrease further. When stimulation was discontinued, both $[K^+]_e$ and ECS volume returned to their original values with a similar time course. After the end of stimulation, the ECS showed a rapid and complete recovery to its pre-stimulation volume. The post-stimulation K^+ undershoot below the baseline, due to the uptake of K^+ by activation of the Na/K pump (Kříž et al., 1975) and glial spatial buffering (Orkand et al., 1966; Syková and Orkand, 1980; Coles and Orkand, 1983), was accompanied by an increase in α of about 6%. λ was not increased during 5 min of stimulation; however, a clear increase of about 0.05 did occur during 30 min of stimulation (Fig. 4F).

The stimulation-evoked $[K^+]_e$ changes in the FT (Fig. 4C) were maximal at 30 Hz. The stimulation produced an increase in $[K^+]_e$ of about 1–4 mM. The rise in $[K^+]_e$ diminished in the rostro-caudal direction, and there were no differences if the VIII. or IX. dorsal root was stimulated. When stimulation continued, $[K^+]_e$ began to decrease more rapidly than in spinal cord; it decreased below its baseline already during stimulation, suggesting that K^+ redistribution is more efficient in the FT than in

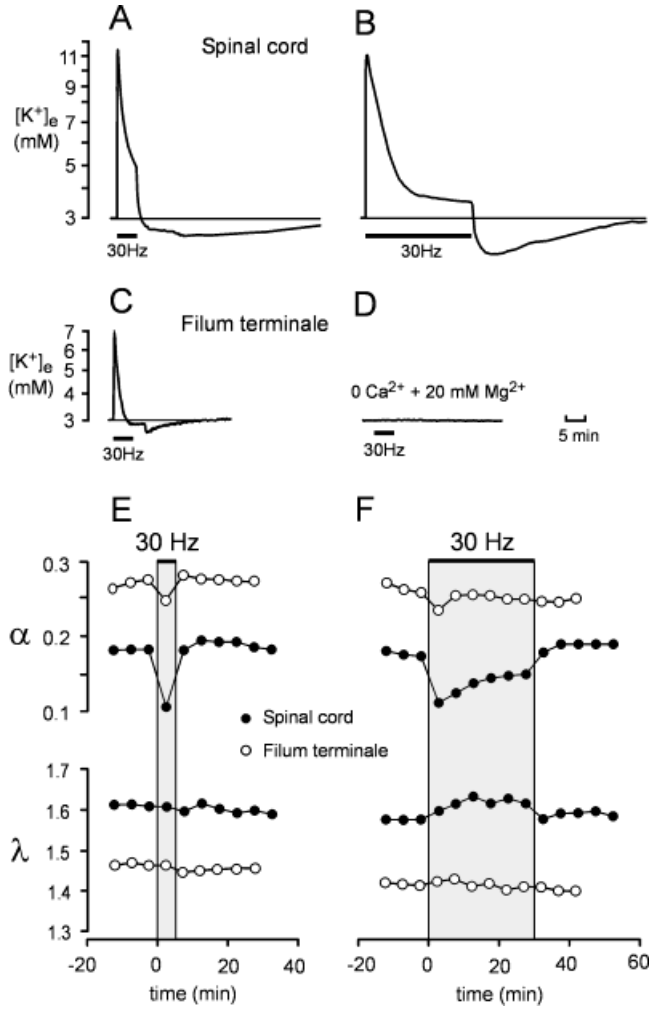

Fig. 4. Effect of repetitive electrical stimulation on changes in $[K^+]_e$ in spinal dorsal horn and filum terminale I. Changes in $[K^+]_e$ in the dorsal horn of the spinal cord evoked by the 30 Hz/5 min (**A**) and 30 Hz/30 min (**B**) stimulation of the VIII dorsal root. In the FT (**C**), a stimulation of 30 Hz/5 min of the VIII dorsal root evoked much smaller changes in $[K^+]_e$ than in the spinal cord (A). The $[K^+]_e$ undershoot below the original K^+ baseline was already present during stimulation. Blocking of synaptic activity by the application of 20 mM Mg^{2+} in Ca^{2+}-free Ringer solution completely inhibited the stimulation-evoked increase in $[K^+]_e$ (**D**). **E**,**F:** Effect of repetitive electrical stimulation (30 Hz) on ECS diffusion parameters in spinal dorsal horn and filum terminale I. The α and λ were recorded at 5 min intervals; the stimulation at a frequency of 30 Hz lasted 5 (E) or 30 min (F). In the spinal dorsal horn the changes in α corresponded to the stimulation-evoked increase in $[K^+]_e$. There were not significant changes in λ. In the filum terminale, α decreased only at the beginning of stimulation, corresponding to the stimulation-evoked increase in $[K^+]_e$, and there were no changes in λ.

the spinal cord. Correspondingly, α decreased only at the beginning of the stimulation when K^+ is elevated; its increase did not exceed 9% and there were no changes in λ. Tetanic stimulation at 30 Hz for 5 or 30 min (Fig. 4E,F) evoked in the FT I an ECS volume decrease from about 0.27 to 0.24 during the first 30 sec; when the stimulation continued and $[K^+]_e$ rapidly returned to resting levels, α also rapidly returned to control values.

It has been shown in our previous experiments on frog spinal cord (Syková and Vyklický, 1977) that the block of synaptic transmission decreases the stimulation-evoked release of K^+ in spinal cord by 85%, and that the remaining 15% of the $[K^+]_e$ increase is a consequence of K^+ released presynaptically from primary afferent fibers and presynaptic terminals. Blocking synaptic transmission with Ca^{2+}-free Ringer solution containing 20 mM Mg^{2+} (Fig. 4D) completely blocked the $[K^+]_e$ rise in the FT. This suggests that the stimulation evoked $[K^+]_e$ increase in FT results only from postsynaptic membranes.

DISCUSSION

From TMA^+ measurements it is known that in all mammalian brain and spinal cord regions, α varies between 0.17–0.26 and λ in isotropic regions is about 1.5–1.6 (Syková, 1997; Nicholson and Syková, 1998). Previously, our measurements in frog were done only in the spinal cord and could only show relative changes in the ECS volume during electrical stimulation of dorsal roots (Syková, 1987). The ECS diffusion parameters in the filum terminale have not been studied previously. Our present results show that the grey matter of the isolated frog spinal cord has similar diffusion parameter values as the isolated rat spinal cord (Prokopová et al., 1997) or rat spinal cord in vivo (Syková et al., 1994). Previous studies also revealed that changes in ECS diffusion parameters are the same in vivo and in isolated spinal cord, although they are somewhat different in slice preparations, where smaller changes in tortuosity usually occur (for further discussion see Syková et al., 1999). The values found in isolated frog spinal cord and filum terminale under high potassium and hypotonic stress resemble those found during similar experimental manipulations in isolated rat spinal cord (Syková et al., 1999) and in vivo in rat during pathological states, e.g., anoxia (Syková et al., 1994). There can also be more subtle interspecies and regional differences, however, that have not yet been depicted. The previous studies performed on rat brain slices (Pérez-Pinzón et al., 1995) or in isolated turtle cerebellum (Krizaj et al., 1996) using hypoosmotic solutions also revealed smaller changes in tortuosity than in high potassium solutions and are therefore in agreement with our study.

Despite the similarities in diffusion and structure of the ECS, mammalian and amphibian astrocytes show morphological differences. Amphibian astrocytes in the spinal cord, as revealed by horseradish peroxidase staining, are radially oriented with their cell bodies located in the grey matter and one or two principal processes extending to the pial surface (Miller and Liuzzi, 1986). Using the patch-clamp method and Lucifer Yellow staining, however, the membrane as well as morphological properties of frog spinal cord cells were found to be similar to those described in rat spinal cord (Chvátal et el., 1995; Chvátal, Anděrová, Syková, unpublished results). GFAP staining in the frog spinal cord shows a dense network formed by thin processes. As compared to the spinal cord, in FT the

network was less dense; however, the overall GFAP staining was more pronounced, and the astrocyte bodies were more densely stained and showed thicker processes.

The different diffusion properties of the two regions obviously reflect their different morphology. In the FT, a structure with glia but a drastically reduced neuropil and a marked decrease in the number of myelinated fibers (Glusman et al., 1979; Gonzáles-Robles and Glusman, 1979; Chesler and Nicholson, 1985), α is significantly higher by about 58%, as compared to the spinal cord. Studies of Glusman et al. (1979), in which DNA content was measured, revealed that the spinal cord has roughly three times the cellular density of the FT. The ECS of the FT measured as the [^{3}H] inulin space was found to be larger by 25% (Glusman et al., 1979), or by 34% (Ritchie et al., 1981), than that of the spinal cord, i.e., somewhat less than in our studies. λ was lower in FT than in spinal cord that corresponds to our finding that astrocytes in the FT have less numerous, although thicker, processes, resembling mammalian glial precursor cells (Chvátal et al., 1995). The diffusion of a particular substance in a tissue is hindered not only by a decrease in the ECS volume fraction, but also by an increase in tortuosity resulting from additional diffusion barriers, imposed by glial maturation (Prokopová et al., 1997) or astrogliosis (Syková et al., 1999). Similar to the developing rat spinal cord when the majority of astrocytes have shorter, less numerous processes and λ is lower than in adult rats, the observed λ in FT is also reduced (Fig. 2 and 3). We cannot, however, exclude the possibility that differences in the extracellular matrix (ECM) of the FT and spinal cord contribute to the observed results, as it has been shown that a decrease in ECM accompanies a decrease in tortuosity in rat hippocampus during astrogliosis and aging (Syková et al., 1998).

High potassium leads to membrane depolarization of various nerve cells and to an increase in cell volume, that results from a net KCl uptake via Na-K-2Cl co-transport and concomitant water influx into astrocytes as well as changes in the Donnan equilibrium (Walz and Hinks, 1985; Syková et al., 1999). In addition, neuronal swelling could also be evoked by a rise in $[K^+]_e$ as a consequence of an increase in excitability and transmitter release produced by depolarization (Vyklický and Syková, 1981; Dietzel et al., 1989). Clearly, exposure to hypotonic conditions causes a rapid increase in cell volume with a net water influx into the cell as the osmotic pressure equalizes across the cell membrane (Olson and Kimelberg, 1995). The greater K^+-evoked swelling in the filum, with more abundant glial cells than neurones, therefore results in a greater decrease in the ECS volume and a greater increase in tortuosity than in spinal cord. The K^+-evoked swelling of glial processes, that presumably have many K^+ channels, has been suggested to lead to an increase in tortuosity (Syková et al., 1999). Our previous study on the rat spinal cord (Syková et al., 1999) showed that the cellular swelling evoked by high K^+ leads to significantly larger changes in α and in persistent and much greater changes in λ than does hypotonic solution. Moreover, the rise in λ correlates closely with an increase in GFAP staining and astrogliosis. We are aware of the fact that amphibian glia may have, in terms of cell swelling, astrogliosis, potassium channels and regulatory responses to elevated potassium, different properties than do mammalian glia (Ritchie et al., 1981) and that the ECS diffusion parameters can differ from those in mammals (Syková et al., 1999).

Studies of Ritchie et al. (1981), using [^{3}H] inulin ECS measurement in the spinal cord and FT at a potassium level of 80 mM, revealed the same relative decrease in ECS volume in both structures, that was only about 35%. Similarly to their findings, we found the changes in α in FT to be about 35%, but they were much smaller than those in spinal cord, that were 53%, probably due to a lower cellular density in FT than in the spinal cord. Our results suggest that approximately ⅔ of cellular swelling may be attributable to glia and ⅓ to neuronal swelling. An increase in tortuosity was present in both frog spinal cord and FT during the application of high K^+, but not in hypotonic solution. This increase in λ during elevated K^+ was significantly higher in the FT, presumably due to a relatively higher ratio between glial cells and neurones than in the spinal cord. This shows that swollen glial cells in FT can form more diffusion barriers than in the complex nervous tissue of the spinal cord. In contrast to mammals, the changes in frog were completely reversible, and there was no persistent increase in tortuosity related to astrogliosis as was found in rat (Syková et al., 1999).

Blocking synaptic transmission eliminated fully the stimulation evoked $[K^+]_e$ rise in FT. This suggests that the stimulation-evoked increase in $[K^+]_e$ results from postsynaptic neurones. The rise of $[K^+]_e$ in the intermediate regions of FT therefore come from sparse neurones and from axons that are mostly present laterally. We can assume more rapid diffusion of K^+ in large ECS of FT. A presence of neurons in the FT (see also Chesler and Nicholson, 1985) was recently verified using patch-clamp method (Chvátal, Anděrová, Syková, unpublished results).

The activity-related decrease in the ECS volume may be partly explained by an increase in glial cell volume owing to K^+ uptake (Walz and Mukerji, 1988) and a K^+ shift mediated by the spatial buffer mechanism (Syková et al., 1988). In our experiments, the increase in $[K^+]_e$ produced by the stimulation of afferent fibers caused a decrease in the ECS volume. Both the $[K^+]_e$ and ECS volume changes had a similar time course and were greater in the spinal cord than in FT. This can be explained by the fact that more K^+ is released by neurones into a smaller ECS volume in spinal cord than in FT. The activity-related decrease in ECS volume fraction is therefore proportional to an elevated $[K^+]_e$ level. It results particularly from the swelling of glial cells, their bodies as well as their processes, although some swelling of neurons may also occur. The tortuosity increase, however, is mainly caused by swollen glial cell processes, that form more diffusion barriers in the FT than in the spinal cord.

REFERENCES

Chesler M, Nicholson, C. 1985. Organization of the filum terminale in the frog. J Comp Neurol 239:431–444.

Chvátal A, Jendelová P, Kříž N, Syková E. 1988. Stimulation-evoked changes in extracellular pH, calcium and potassium activity in the frog spinal cord. Physiol Bohemoslov 37:203–212.

Chvátal A, Pastor A, Mauch M, Syková E, Kettenmann H. 1995. Distinct populations of identified glial cells in the developing rat spinal cord: Ion channel properties and cell morphology. Eur J Neurosci 7:129–142.

Coles JA, Orkand RK. 1983. Modification of potassium movement through retina of the drone (*Apis mellifera*) by glial uptake. J Physiol (Lond) 340:157–174.

Dietzel I, Heinemann U, Lux HD. 1989. Relations between slow extracellular potential changes, glial potassium buffering, and electrolyte and cellular volume changes during neuronal hyperactivity in cat brain. Glia 2:25–44.

Friedman B, Hockfield S, Black JA, Woodruff KA, Waxman SG. 1989. In situ demonstration of mature oligodendrocytes and their processes: an immunocytochemical study with a new monoclonal antibody, Rip. Glia 2:25–44.

Fuxe K, Agnati LF. 1991. Volume transmission in the brain: novel mechanisms for neural transmission. New York: Raven Press.

Glusman S, Pacheco M, Gonzáles Robles A, Haber B. 1979. The filum terminale of the frog spinal cord, a non transformed glial preparation: I. morphology and uptake of γ-aminobutyric acid. Brain Res 172:259–276.

Gonzáles-Robles A, Glusman S. 1979. The filum terminale of the frog spinal cord. Cell Tissue Res 199:519–528.

Kimelberg HK, Frangakis MV. 1985. Furosemide- and bumetanide-sensitive ion transport and volume control in primary astrocyte cultures from rat brain. Brain Res 361:125–134.

Kimelberg HK, Ransom BR. 1986. Physiological and pathological aspects of astrocyte swelling. In: Federoff S, Vernadakis A, editors. Astrocytes: cell biology and pathology of astrocytes. New York: Academic Press. p 129–166.

Kříž N, Syková E, Vyklický L. 1975. Extracellular potassium changes in the spinal cord of the cat and their relation to slow potentials, active transport and impulse transmission. J Physiol (Lond) 249:167–182.

Krizaj D, Rice ME, Warde RA, Nicholson C. 1996. Water compartmentalization and extracellular tortuosity after osmotic changes in cerebellum of *Trachemys scripta*. J Physiol (Lond) 492:887–896.

Miller RH, Liuzzi FJ. 1986. Regional specialization of the radial glial cells of the adult frog spinal cord. J Neurocytol 15:187–196.

Nicholson C, Phillips JM. 1981. Ion diffusion modified by tortuosity and volume fraction in the extracellular microenvironment of the rat cerebellum. J Physiol (Lond) 321:225–257.

Nicholson C, Syková E. 1998. Extracellular space structure revealed by diffusion analysis. Trends Neurosci 21:207–215.

Olson JE, Kimelberg HK. 1995. Hypoosmotic volume regulation and osmolyte transport in astrocytes is blocked by an anion transport inhibitor, L-644,711. Brain Res 682:197–202.

Orkand RK, Nicholls JG, Kuffler SW. 1966. Effect of nerve impulses on the membrane potential of glial cells in the central nervous system of Amphibia. J Neurophysiol 70:788–806.

Pérez-Pinzón MA, Tao L, Nicholson C. 1995. Extracellular potassium, volume fraction, and tortuosity in rat hippocampal CA1, CA3 and cortical slices during ischemia. J Neurophysiol 74:565–573.

Prokopová Š, Vargová L, Syková E. 1997. Heterogeneous and anisotropic diffusion in the developing rat spinal cord. Neuroreport 8:3527–3532.

Ritchie T, Packey DJ, Trachtenberg MC, Haber B. 1981. K^+-induced ion and water movements in the frog spinal cord and filum terminale. Exp Neurol 71:356–369.

Roitbak T, Syková E. 1999. Diffusion barriers evoked in the rat cortex by reactive astrogliosis. Glia 28:40–48.

Svoboda J, Motin VG, Hájek I, Syková E. 1988. Increase in extracellular potassium level in rat spinal dorsal horn induced by noxious stimulation and peripheral injury. Brain Res 458:97–105.

Svoboda J, Syková E. 1991. Extracellular space volume changes in the rat spinal cord produced by nerve stimulation and peripheral injury. Brain Res 560:216–224.

Syková E. 1987. Modulation of spinal cord transmission by changes in extracellular K^+ activity and extracellular volume. Can J Physiol Pharmacol 65:1058–1066.

Syková E. 1997. The extracellular space in the CNS: its regulation, volume and geometry in normal and pathological neuronal function. Neuroscientist 3:334–347.

Syková E, Mazel T, Šimonová Z. 1998. Diffusion constrains and neuron-glia interaction during aging. Exp Gerontol 33:837–851.

Syková E, Orkand RK. 1980. Extracellular potassium accumulation and transmission in frog spinal cord. Neuroscience 5:1421–1428.

Syková E, Orkand RK, Chvátal A, Hájek I, Kříž N. 1988. Effect of carbon dioxide on extracellular potassium accumulation and volume in isolated frog spinal cord. Pflügers Arch 412:183–187.

Syková E, Shirayev B, Kříž N, Vyklický L. 1976. Accumulation of extracellular potassium in the spinal cord of frog. Brain Res 106:413–417.

Syková E, Svoboda J, Polák J, Chvátal A. 1994. Extracellular volume fraction and diffusion characteristics during progressive ischemia and terminal anoxia in the spinal cord of the rat. J Cereb Blood Flow Metab 14:301–311.

Syková E, Vargová L, Prokopová Š, Šimonová Z. 1999. Glial swelling and astrogliosis produce diffusion barriers in the rat spinal cord. Glia 25:56–70.

Syková E, Vyklický L. 1977. Changes of extracellular potassium activity in isolated spinal cord of frog under high Mg^{2+} concentration. Neurosci Lett 4:161–165.

Van Harreveld A, Khattab FI. 1967. Changes in cortical extracellular space during spreading depression investigated with the electron microscope. J Neurophysiol 30:911–929.

Vyklický L, Syková E 1981. Effect of increased extracellular potassium activity in the frog spinal cord on the flexor reflex. In: Syková E, Hník P, Vyklický L, editors. Ion-selective microelectrode and their use in excitable tissues. New York: Plenum Press. p 195–200.

Walz W, Hinks EC. 1985. Carrier-mediated KCl accumulation accompanied by water movements is involved in the control of physiological K^+ levels by astrocytes. Brain Res 343:44–51.

Walz W, Mukerji S. 1988. KCl movements during potassium-induced cytotoxic swelling of cultured astrocytes. Exp Neurol 99:17–29.

Zoli M, Jansson A, Syková E, Agnati LF, Fuxe K 1999. Volume transmission in the CNS and its relevance for neuropsychopharmacology. TiPS 20:142–150.